Chalcogenide Letters Vol. 9, No. 12, December 2012, p. 483 - 493

STUDY OF THE LINEAR OPTICAL PROPERTIES AND SURFACE ENERGY LOSS OF 5',5"-DIBROMO-O-CRESOLSULFOPHTHALEIN THIN FILMS

HUSSAIN A. BADRAN*, MOHAMMED F. AL-MUDHAFFER, QUSAY M. A. HASSAN, ALAA Y. AL-AHMAD
Department of Physics, College of Education, University of Basrah, Basrah, Iraq

The optical constants such as (refractive index *n*, extinction coefficient *k* and absorption coefficient *α*) were calculated for 5',5"-dibromo-o-cresolsulfophthalein (BCP) thin films by using spectrophotometer measurements of the transmittance, absorbance and reflectance at normal incidence in the spectral range 350–900 nm. The obtained values of both *n* and *k* were found to be dependent of the film thicknesses. The refractive index has anomalous behaviour in the wavelength range 350–900 nm besides a high energy transition at 2.385 eV. The optical parameters (dispersion energy E_d, oscillation energy E_o and the high frequency dielectric constant ε_∞) were calculated using Wemple and Didomenico method. The volume energy loss (VELF) and the surface energy loss (SELF) functions are also investigated.

(Received November 13, 2012; Accepted December 7, 2012)

Keywords: Optical constants, energy loss, electrical conductivity, Tin films.

1. Introduction

Optical properties of thin films have been the subject of intense study during the last decades and great efforts have been made to develop the mathematical formulation describing the transmittance and reflectance of different optical systems [1,2]. Among the existing methods for determining the optical constants of those based exclusively on the optical transmission spectra at normal incidence have been applied to different crystalline and amorphous materials deposited on transparent substrates in the form of thin films [3-7].

The study of the optical constants of materials has been interesting for many reason. First, the use of materials in optical fibres and reflected coating requires accurate knowledge of their optical constants over wide range of wavelength, second, the optical properties of all materials are related to their atomic structure, electronic band structure and electrical properties. The structural bonding between the neighbours determines the optical properties, such as absorption and transmission of the amorphous material [8].

In the present work we determine the optical constant and dispersion parameters also the volume energy loss (VELF), surface energy loss (SELF) functions for 5',5"-dibromo-o-cresolsulfophthalein (BCP) thin films with deferent thickness. The optical properties of thin films were determined by using transmission, absorbance and reflection data spectrum in the wavelength range 350-900nm.

2. Materials and preparation

5',5"-dibromo-o-cresolsulfophthalein (BCP), with molecular mass= 540.22 g mol^{-1}, has been selected for our experiments as shown in Fig. 1.BCP dye was supplied from Aldrich Company with purity 96%. In our experiment, the host material is Poly (methyl methacrylate) (PMMA) and the ratio of dyes in PMMA by weight is 0.05, 0.1, 0.2 and 0.4 respectively.

---

*Corresponding author: badran_hussein@yahoo.com

The dye-doped PMMA films were prepared as follows: dye and PMMA are dissolved separately in chloroform and then the solution of dye and that of PMMA are mixed, heated (up to 50°C) and stirred for 2 hr, thus the mixed sols of dye and PMMA were obtained. After the sols were filtrated, the films were prepared on a clean glass slide by the repeat-spin-coating method and dried at room temperature (300K) for 48 hr. The thickness of the films are about C1=306.8, C2=386.7, C3=550.4 and C4=605.9 nm respectively and the film samples have good purity and uniform thickens. The optical absorption spectra are recorded from 350 to 900 nm in steps of 2 nm using Cecil Reflecta-Scan CE -3055 Reflectance Spectrometer at room temperature. The absorbance spectra of samples with different thicknesses are shown in Fig. 2. The optical absorptions is found to increase with increasing wavelength until it reaches 400nm. For λ > 400 it is decreasing with increasing wavelength. For λ > 600 it's the same for all samples.

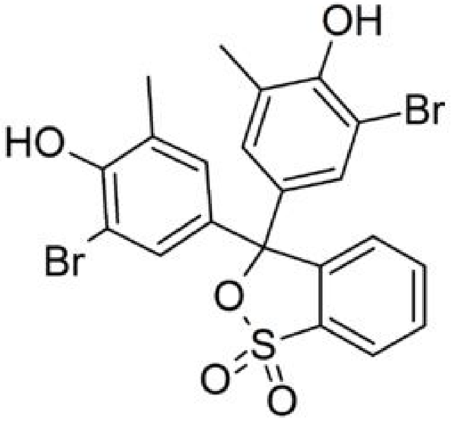

Fig.1. The chemical structure of BCP dye
different

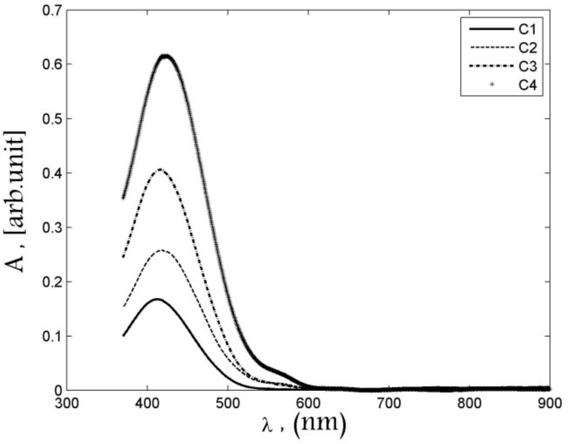

Fig.2 Absorbance spectra of thin films deposited at
concentrations.

3. Results and discussion

3.1. Optical absorption edge of the thin films

The transmittance spectra of the thin films are shown in Fig.3. The transmission through the film is relatively low at below band gap region, indicating high concentration of defects, free carriers. The transmittance decreases abruptly in the short wavelengths which is due to the band edge absorption. Fig. 4 shows the reflection spectrum of the samples. It is observed from Fig. 4 that reflection decreases with the increase in wavelength. A sudden decrease at a particular wavelength, indicates the presence of optical band gap in these samples.

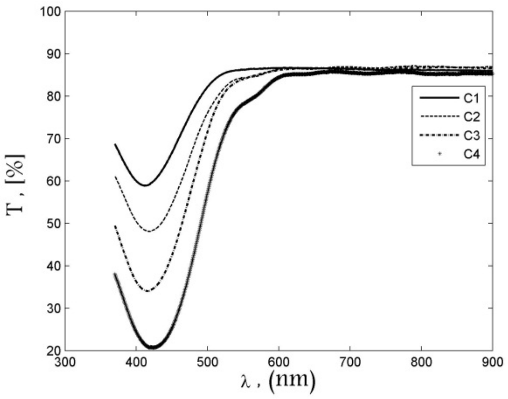

Fig. 3. Optical transmission of the thin films deposited at different concentrations.

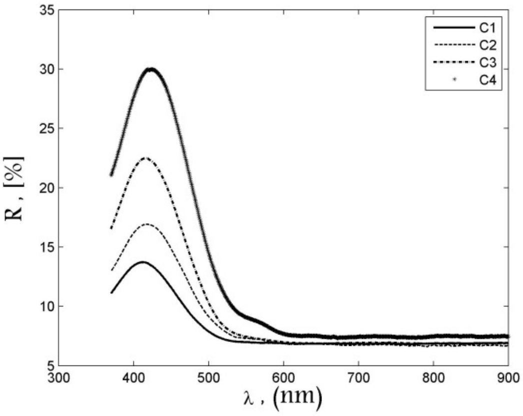

Fig. 4. Optical reflection of the thin films deposited at different concentrations.

The incoming photons have sufficient energy to excite electrons from the valence band to the conduction band, resulting in strong absorption in sample. The optical absorption edge was determined by the optical absorption, a simple method that provides explanation for the features concerning the band structure of the film. The optical absorption edge was analyzed by the following relationship (Tauc's Procedure) [9].

$$\alpha = \frac{A}{h\nu}(h\nu - E_g)^m \tag{1}$$

where α is absorption coefficient, A is an energy-independent constant and E_g is the optical band gap. The exponent m depends on the nature of the transition, m= 1/2, 2, 3/2 or 1/3 for allowed direct, allowed indirect, forbidden direct or forbidden indirect transitions, respectively. Eq.1 can be written as

$$\frac{d[\ln(\alpha h\nu)]}{d(h\nu)} = \frac{m}{h\nu - E_g} \tag{2}$$

The type of transition can be obtained by determining the value of m. A discontinuity in the $d[\ln(\alpha h\nu)]/d(h\nu)$ versus $h\nu$ plot at the band gap energy, i.e. at $h\nu = E_g$ can be observed. The discontinuity at a particular energy value gives the band gap, E_g [10]. The curves of $\ln(\alpha h\nu)$ versus $\ln(h\nu - E_g)$ were plotted using the E_g value to determine m value and it was found about 2 from the slope of plotted curves. Thus, obtained m value suggests that the fundamental absorption edge in the films is formed by the indirect allowed transitions. In the transition process, the total energy and momentum of the electron-photon system must be conserved. Fig.5. shows the plots of $(\alpha h\nu)^2$ versus $h\nu$ of the films. The values of the indirect optical band gap E_g are given in Table 1.

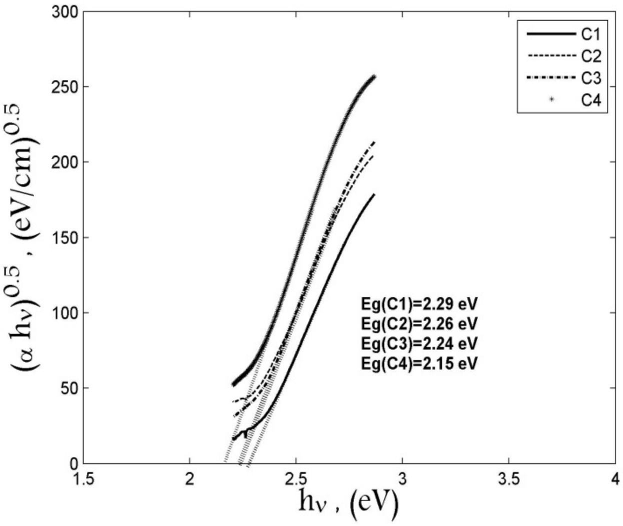

Fig.5. $(\alpha h\nu)^{0.5}$ *vs. photon energy of thin films at different concentrations .*

.

The optical band gap values obtained by this method are suitable for many scientific studies and technological applications, such as gas sensors, and piezoelectric devices. As seen from Table 1, the dye concentrations lead to a decrease in optical band gaps of the films. These results show that the dye concentrations cause shrinkage in the optical absorption edge and therefore change in the band structure of the films. This suggests that the defects in thin films take place during formation of the films. It is also noted to discussion that the decrease in energy band gap increases the width of the energy bands. The decrease in the width of the energy band induces to move the band edge of the conduction band downward and that of the valence band upward [11].

Table 1 The optical band gap of the thin films for different concentrations.

Thickness(nm)	$E_g^{ind}(eV)$
C1=306.8	2.29
C2=386.7	2.26
C3=550.4	2.24
C4=605.9	2.15

3.2. Optical dispersion characteristics

The refractive index (n) of the films are determined by reflection spectra in the wavelength range 350–900 nm by Reflectophotometer at room temperature and we calculated the refractive index values of the films using the following equation [12].

$$n = \left(\frac{1+R}{1-R}\right) + \sqrt{\frac{4R}{(1-R)^2} - k} \tag{3}$$

where R is the reflectance and $k = (\lambda\alpha/4\pi)$ is the extinction coefficient. The refractive index ,n, and extinction coefficient k dependence of the wavelength are shown in Figs. 6 and 7. As seen in Figs. 6 and 7 n and k values are influenced by decrease the concentrations and increase with decreasing the wavelength up to 400 nm after that will decrease with decreasing the wavelength. Therefore, they show the normal dispersion.

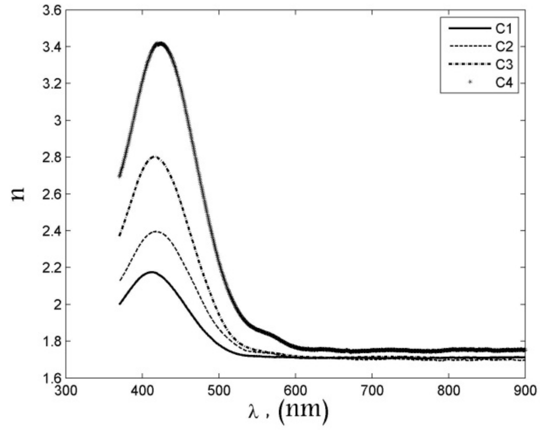

Fig. 6. Dispersion curves of refractive index n for the films as a function of wavelength.

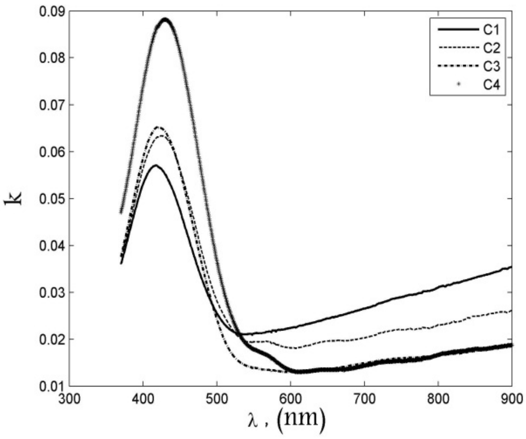

Fig. 7. Dispersion curves of extinction coefficient k for the films as a function of wavelength .

3.3 Dispersion Parameters

Wemple and Didomenico [13,14] use a single-oscillator description of the frequency-dependent dielectric constant to define a “dispersion energy” parameters E_d and E_o. The refractive index dispersion of the films studied can be fitted by Wemple and Didomenico. The dispersion plays an important role in the research for optical materials, because it is a significant factor in optical communication and in designing devices for spectral dispersion. Although these rules are quite different in detail, one common feature is the over-whelming evidence that both crystal structure and ionicity influence the refractive index behaviour of solids in ways that can be simply described [15].

The relation between the refractive index *n*, and the single oscillator strength below the band gap is given by the expression [13,14]:

$$(n^2-1)^{-1} = \frac{E_0}{E_d} - \frac{1}{E_0 E_d}E^2 \tag{4}$$

where E is the photon energy, E_o is the oscillator energy and E_d is the dispersion energy. A plot of $(n^2-1)^{-1}$ versus E^2 of the films at different thicknesses are illustrated in Fig. 8. It is clear that, the refractive index declines towards the longer wavelengths due to the influence of films absorption. The values of E_d and E_o were obtained from the slope and the intersection obtained from extrapolation of the line to zero photo energy and are given in the Table 2.

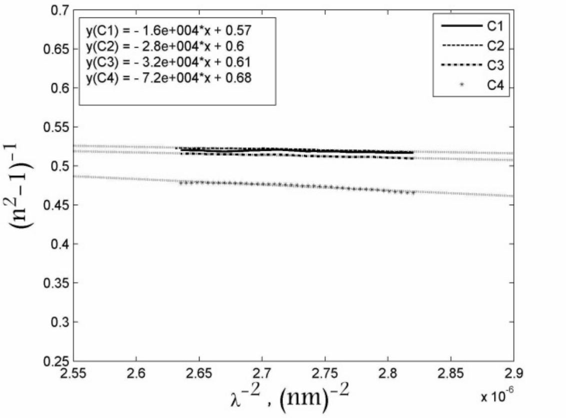

Fig.8. $(n^2-1)^{-1}$ *vs.* $(h\nu)^2$ *at different concentrations.*

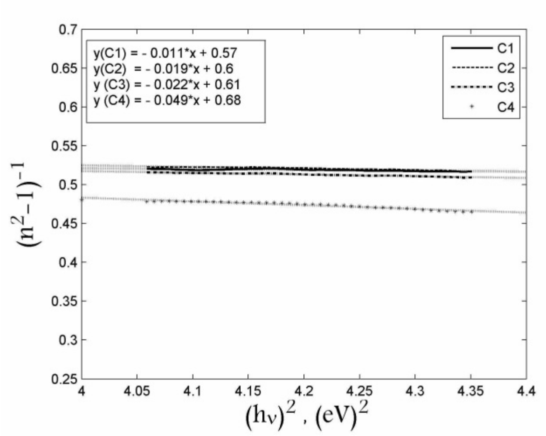

Fig.9. $(n^2-1)^{-1}$ *vs.* λ^{-2} *at different concentrations.*

The dielectric constant of a material could be calculated using the dispersion relation of incident photon. The refractive index was also fitted using a function for extrapolation towards shorter wavelengths [14]. The model of Moss [16] stated that the free carriers contribution to dispersion are relatively small. This means that data corresponding to the wavelength range lying below the absorption edge of the material are to be used. In such a case, so, one can apply the next relation. The properties of the investigated sample could be treated as a single oscillator at wavelength λ_0 at high frequency. The high frequency dielectric constant can be calculated by applying the following simple classical dispersion relation [16]:

$$\frac{n_0^2-1}{n^2-1}=1-\left(\frac{\lambda_0}{\lambda}\right)^2 \tag{5}$$

where n_0 is the refractive index at infinite wavelength λ_0 (average interband oscillator wavelength), n the refractive index and λ the wavelength of the incident photon. Plotting $(n^2-1)^{-1}$ against λ^{-2} which showed linear part, was below the absorption edge as shown in Fig.9. Values of n_0 for thin films are given in Table 2. Equation 5 can also be written as [18]:

$$n^2-1=\left(\frac{S_0^2\lambda_0^2}{1-(\lambda^2/\lambda_0^2)}\right) \tag{6}$$

where S_o is the average oscillator strength which equals to:

$$S_0=\frac{n_0^2-1}{\lambda_0^2} \tag{7}$$

The S_o values for the films were calculated using equation 6 and are given in Table 2.

The M_{-1} and M_{-3} moments of the optical spectra can be obtained from the relationship [17,19]

$$E_{\circ}^2=\frac{M_{-1}}{M_{-3}} \qquad \text{and} \qquad E_d^2=\frac{M_{-1}^3}{M_{-3}} \tag{8}$$

The obtained values are given in Table 2. The M_{-1} and M_{-3} moments changed due to the formation coordination of complex. It is found that M_{-1} values decrease with increasing the thickness of film.

Table 2: Effective oscillator model parameters of samples of different concentrations.

Thickness(nm)	**E_o(eV)**	**E_d(eV)**	**M_{-1}**	**M_{-3} (eV)^2**	**n_0**	**λ_0(nm)**	**S_0 x10^{-13} (m^{-2})**
C1=306.8	5.79	10.15	1.75	0.033	1.65	167.54	6.25
C2=386.7	5.61	9.36	1.66	0.052	1.63	216.02	3.57
C3=550.4	5.26	8.63	1.63	0.059	1.62	229.03	3.12
C4=605.9	3.72	5.47	1.47	0.106	1.57	325.39	1.38

3.4. Dielectric characterizations

It is well-known that polarizabiltiy of any solid is proportional to its dielectric constant. The real and imaginary parts of the complex dielectric constant are expressed as [12]:

$$\varepsilon_1=n^2-k^2 \qquad \text{and} \qquad \varepsilon_2=2nk \tag{9}$$

where ε_1 and ε_2 are the real and imaginary parts of the dielectric constant, respectively. The dependences of ε_1 and ε_2 on the photon energy are shown in Figs. 10 and 11. The real and imaginary parts of the dielectric constant follow the same pattern and the values of the real part are higher than the imaginary part. The variation of the dielectric constant with the photon energy indicates that some interactions between photons and electrons in the films are produced in this energy range. These interactions are observed on the shapes of the real and imaginary parts of the dielectric constant and they cause the formation of peaks in the dielectric spectra which depends on the material type.

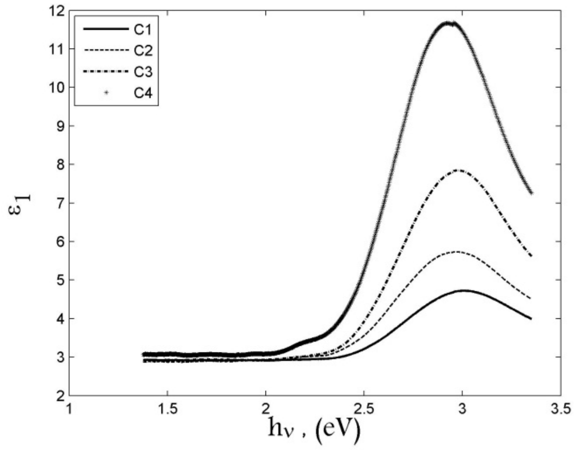

Fig. 10. The variation of ε_1 *with the photon energy for different concentrations.*

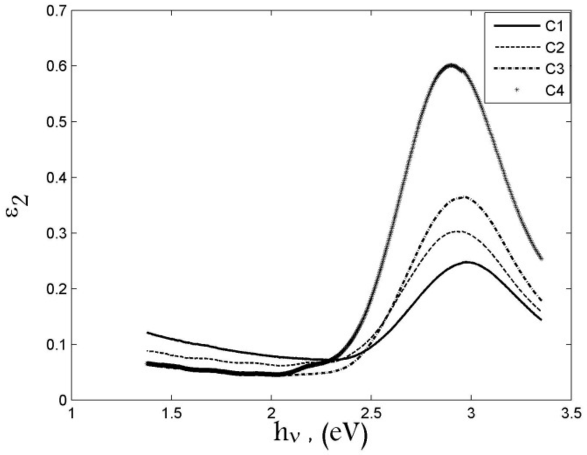

Fig. 11. The variation of ε_2 *with the photon energy for different concentrations.*

3.5. Optical and electrical conductivity of thin films

The absorption coefficient α can be used to calculate the optical and electrical conductivity σ_{opt} , σ_e as follow [25]:

$$\sigma_{opt} = \frac{\alpha n c}{4\pi} \tag{10}$$

$$\sigma_e = \frac{2\lambda\sigma_{opt}}{\alpha} \tag{11}$$

where c is the velocity of light.

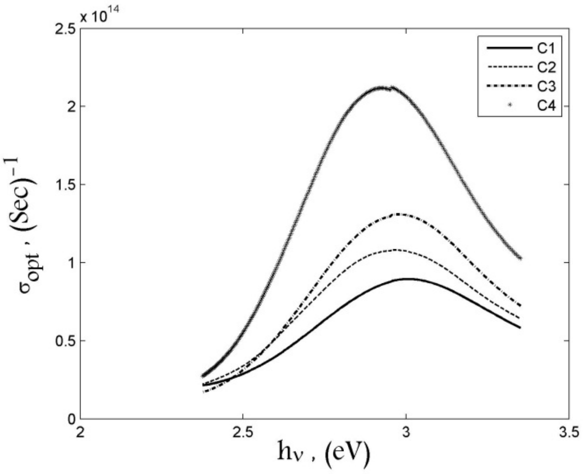

Fig. 12. optical conductivity versus hv *for different concentrations .*

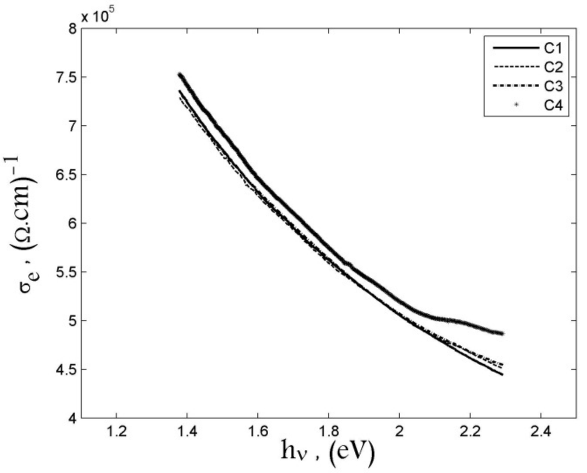

Fig. 13. electrical conductivity versus hv *for different concentrations.*

Figs.12 and 13 shows the variation of optical conductivity σ_{opt} and electrical conductivity σ_e as a function of photon energy *hv*. It is worthwhile to note that the dye inclusion has greatly reduced the dielectric constant and increased the optical conductivity. The increased optical conductivity at high photon energies is due to the high absorbance of sample thin films and also may be due to the electron excited by photon energy [26].

3.6. volume energy loss and surface energy loss of thin films:

Quantities of interest in studying the rate of energy loss for electrons passing through a material are the imaginary part of the reciprocal of the dielectric constant, which is known as the volume energy loss (VELF) and the surface energy loss (SELF) functions. They are related to the real and imaginary parts of the dielectric constant by the following relations [21,22] and plotted in Figs.14 and 15.

$$VELF = -lm(\frac{1}{\varepsilon}) = \frac{\varepsilon_2}{\varepsilon_1^2 + \varepsilon_2^2} \tag{12}$$

$$SELF = -lm\left(\frac{1}{\varepsilon + 1}\right) = \frac{\varepsilon_2}{[(\varepsilon_1 + 1)^2 + \varepsilon_2^2]} \tag{13}$$

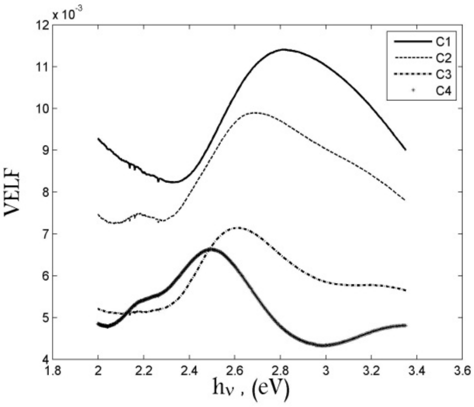

Fig.14. The variation of VELF versus $h\nu$ *for different concentrations* .

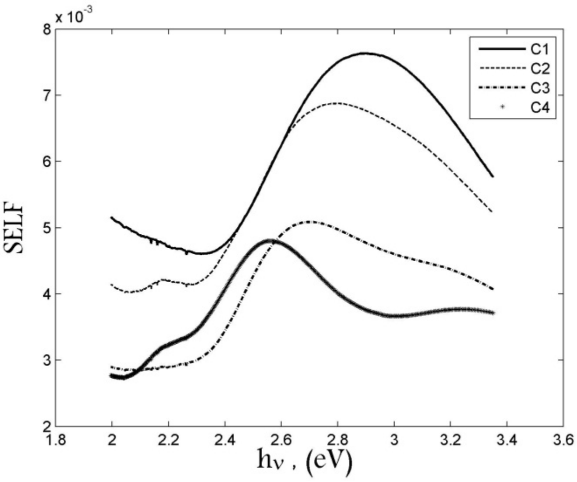

Fig.15. The variation of SELF versus $h\nu$ *for different concentrations* .

From such figures, there is no significant difference between them at lower and higher photon energies it is clear that the volume energy loss is greater than surface energy loss at all incident photon energies.

The interband transition strength J_{cv} accounts for the dipole selection rules for the transitions [23]. J_{cv} is proportional to the probability that a transition of an electron between the filled valence band and the empty conduction band with transition energy takes place and is related to complex dielectric constant (ε) by [24].

$$J_{cv} \equiv \operatorname{Re} J_{cv} + \operatorname{Im} J_{cv} = \frac{4\pi\, m_o^2}{e^2 h^2}\,\frac{E^2}{2}(\varepsilon_2 + i\varepsilon_1) \tag{14}$$

where $\operatorname{Re} J_{cv}$, $\operatorname{Im} J_{cv}$ are the real and imaginary part of interband transition strength, m_o mass of the electron, E is the photon energy, e charge of the electron and h blank constant. J_{cv} is proportional to the transition probability and has units $g.cm^{-3}$. For computational convenience, we take the prefactor ($4\pi^2\, m_o^2 / e^2\, h^2$) in Equation 14, whose value in $8.289 \times 10^{-6}\, g.eV^{-2}$ as unity. The J_{cv} calculated from is Equation 14 are shown in the Figs.16 and 17.

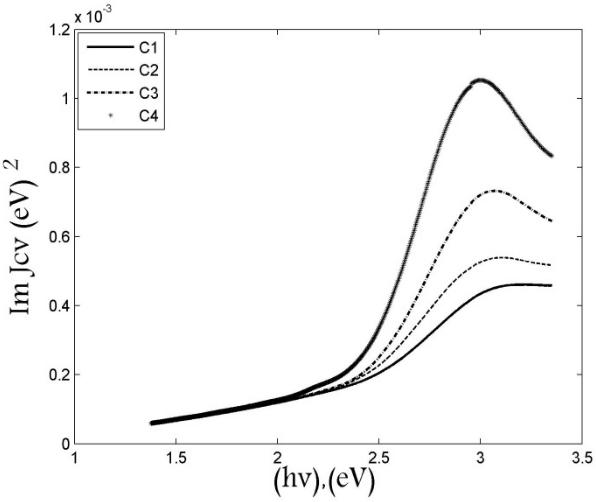

Fig.16.Imaginary part of interband transition strength versus hv for different concentrations.

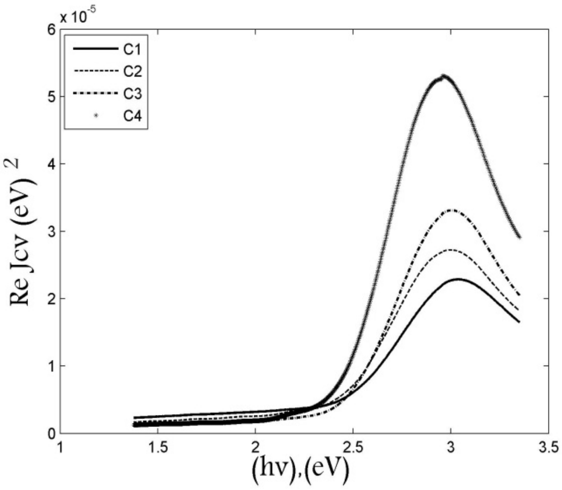

Fig.17.Real part of interband transition strength versus hv for different concentrations.

4. Conclusion

The effect of thicknesses on optical properties of 5',5"-dibromo-o-cresolsulfophthalein (BCP) thin films deposited onto glass substrates by the repeat-spin-coating method has been investigated. The films thicknesses have indirect band gap from 2.29 eV to 2.15 eV. The optical constant such as refractive index, extinction coefficient, high frequency dielectric constant, and dispersion energy are more sensitive to the thin films thicknesses. Both surface and volume energy loss functions have been obtained by depending on real and imaginary parts of dielectric constant, it has maximum peak at energy region $\approx$2.8 eV this leads to single electron excitation process that occurs in the thin films.

References

[1] R.Swane Poel, Phys E: Sci Instrum **17**, 896 (1984).
[2] J.M.Gonzalez Leal,R.Prieto Alcon, M.Stuchlik,M.Vlcek,S.R.Elliott, E.Marquez, Opt.Mater **27** ,147 (2004).
[3] k.A.Aly,A.Dahshan,A.M.Abousehly , Philos Mag.**881**, 47 (2008).
[4] J.C.Manifacier ,J.Gasiot,J.P.Fillard, J. Phys.E:Sci Instrum, **9**,1002 (1976).

[5] R.Swane poel, J.Phys. E: Instrum **16** ,1214 (1983).

[6] M. Hamman , M. A. Harith andW.H .Osman. Solid Commun. **59**, 271 (1986).

[7] J.Kalomiros,A.Spyridelis, J. Phys. Statu Solidi **107**, 633 (1988).

[8] E. Marquez, J. Ramirez Malo, P. Villares, R. Jimenez Garay ,P. J. S. Ewen, A. E. Owen, J. Phys. D: Appl. Phys **25**,535 (1992).

[9] N.F. Mott, E.A. Davis, Electronic Process in Non-Crystalline Materials, Calendron Press, Oxford (1979).

[10] F. Yakuphanoglu, M. Arslan, S.Z. Yıldız, Opt. Mater. **27**, 1153 (2005).

[11] F. Yakuphanoglu, Opt. Mater. **29**, 253 (2006).

[12] F. Abeles (Ed.), Optical Properties of Solids, North-Holland Publishing Company, Amsterdam, London (1972) .

[13] Didomenico M., Wemple S.H., Jo. of Appl. Phys. **40**, 720 (1969)

[14] S.H. Wemple, M. Didomenico, Phys. Rev. **B 3** ,1338 (1971).

[15] J.N. Zemel, J.D. Jensen, R.B. Schoolar, Phys. Rev. A **140** , 330 (1965).

[16] T.S. Moss, Optical Properties of Semiconductors, Butter Worths Scientific Publication LTD., London (1959).

[17] Fahrettin Y., Hilmi E. , Refractive Index Dispersion and Analysis of the Optical Constants of an Ionomer Thin Film , Optica Applicata, XXXV(**4**), 969 (2005).

[18] F. Yakuphanoglu, A. Cukurovali, I. Yilmaz, Physica B **351**, 53 (2004).

[19] S.H. wimple, M. diDomenico, Phys. Rev. Lett. **23**, 1156 (1969).

[20] M.M. El-Nahass, A.M. Farag, K.F. Abd El-Rahman, A.A.A. Darwish, Opt. Laser Technol. **37,** 513 (2005).

[21] M.M. El-Nahass, Z. El-Gohary, H.S. Soliman , Opt. Laser Technol. **35**, 523 (2003).

[22] R. H. Ritchie, Phys. Rev. **106**, 874 (1957).

[23] R. H. French, H. Mullejans , D. J. Jones , J. Am. Ceram. Soc. **81**, 2549 (1998).

[24] R. H. French , J. Am. Ceram. Soc. **83**, 2117 (2000).

[25] J.I. Pankove, Optical Processes in Semiconductors, Dover Publications Inc., New York, (1975) .

[26] F. Yakuphanoglu, A. Cukurovali, I. Yilmaz, Opt. Mater. **27**, 1366 (2005).